

Equatorial ocean dynamics and the undercurrent

7.1. Linearization about a state of rest

Particularly useful approximate solutions of the primitive equations can be obtained by linearizing them about a state of rest and assuming that the background (mean) vertical density structure is horizontally but not vertically uniform. In order to simplify the presentation we shall assume incompressibility and hydrostatic equilibrium which we discussed in earlier lectures. It is possible to drop the first assumption without too much trouble for dealing with the atmosphere but we consider the ocean application here. The momentum equations for small perturbations about the state of rest are

$$(7.1.1) \quad \begin{aligned} \frac{\partial u}{\partial t} - fv &= -\frac{1}{\rho_0} \frac{\partial p}{\partial x} \\ \frac{\partial v}{\partial t} + fu &= -\frac{1}{\rho_0} \frac{\partial p}{\partial y} \\ g\rho &= -\frac{\partial p}{\partial z} \end{aligned}$$

The Coriolis parameter f is $2\Omega \sin \varphi$ where Ω is the angular velocity of the Earth and $\rho_0 = \rho_0(z)$ is the assumed mean density profile. As before the equation of continuity in the incompressible case is

$$(7.1.2) \quad \frac{\partial w}{\partial z} + \frac{\partial u}{\partial x} + \frac{\partial v}{\partial y} = 0$$

If we assume that there are no sources of heat and salinity for the present then the incompressible version of mass conservation implies that $\frac{d\rho}{dt} = 0$. When linearized this becomes

$$(7.1.3) \quad \frac{\partial \rho}{\partial t} + w \frac{\partial \rho_0}{\partial z} = 0$$

7.2. Separation of Variables and the vertical Sturm-Liouville equations

These five equations have the five unknowns (u, v, w, p, ρ) and general solutions are possible. Those of interest to us are separable in the vertical direction. We choose the following separation for the five variables

$$\begin{aligned} \vec{u} &= \hat{u}(z) \vec{U}(x, y, t) \\ p &= \hat{p}(z) \eta(x, y, t) \\ \rho &= \hat{\rho}(z) d(x, y, t) \\ w &= \hat{h}(z) \tilde{w}(x, y, t) \end{aligned}$$

where for reasons that will become clearer later we assume that \hat{u} and \hat{h} have the dimensions of length whereas \hat{p} and $\hat{\rho}$ have their ordinary units (implying, of

course, that the horizontal dependent components are dimensionless). The vertical equations can now be deduced up to a separation constant from the linearized set above. We obtain the four equations for the vertical part of the solutions:

$$(7.2.1) \quad \begin{aligned} \rho_0 \widehat{u} &= \widehat{p}/g \\ g \widehat{\rho} &= \widehat{p}_z \\ \widehat{h}_z &= \widehat{u}/H_0 \\ \widehat{\rho} &= (\rho_0)_z \widehat{h} \end{aligned}$$

where the factor g , the acceleration due to gravity, has been included in the first equation for dimensional consistency and H_0 is the separation constant which has dimension of length. Combining the first and third equations and the second and fourth reduces this to

$$(7.2.2) \quad \begin{aligned} gH_0 \widehat{h}_z &= \widehat{p}/\rho_0 \\ \widehat{p}_z &= g(\rho_0)_z \widehat{h} \end{aligned}$$

and this is easily condensed further to

$$(7.2.3) \quad \frac{1}{\rho_0} (\rho_0 \widehat{h}_z)_z + \frac{N^2}{c_e^2} \widehat{h} = 0$$

where $N \equiv (-g\rho_0^{-1}(\rho_0)_z)^{1/2}$ is termed the Brunt-Vaisala frequency and measures the stability of the background stratification. Note that is always real if the density profile is stable. Parcels of fluid displaced within a density stratification will tend to oscillate at this frequency due to buoyancy effects. The separation constant has been “renamed” $c_e^2 \equiv gH_0$ where c_e is referred to as shallow water speed for reasons that will become clearer later. The reason for assuming that c_e^2 is positive is because the operator $H = \frac{-1}{\rho_0 N^2} \partial_z \rho_0 \partial_z$ may easily be shown to be positive providing that the stratification is stable and hence has the positive eigenvalues c_e^{-2} . For the ocean the lower boundary condition is that the vertical velocity vanishes and so

$$(7.2.4) \quad \widehat{h}(0) = 0$$

At the ocean surface the hydrostatic relation shows that the pressure near the unperturbed surface L is

$$p \approx \rho_0(L)gz + p_0$$

where z is the perturbation vertical displacement and p_0 is constant (exercise). Differentiating this with respect to time gives us the upper boundary condition

$$(7.2.5) \quad \rho_0(L)g\widehat{h}(L) = \widehat{p}(L)$$

Equations (7.2.3), (7.2.4) and (7.2.5) together with the assumption that $N > 0$ form a Sturm-Liouville eigensystem. The mathematical literature on such systems is extensive and the eigenvalues c_e^2 can be shown to be discrete, bounded above, and, as already noted, positive. To a high degree of accuracy in the ocean

$$(7.2.6) \quad \frac{-1}{\rho_0 N^2} \partial_z \rho_0 \partial_z = \frac{-1}{N^2} \partial_{zz}$$

and so we can see that the eigenvalues and eigenvectors are determined by the vertical profile of the Brunt-Vaisala frequency. The eigenvectors in this system are called the *normal, vertical or baroclinic/barotropic modes*. The applications of

these modes are very extensive particularly in ocean dynamics. The mode with the greatest eigenvalue and the simplest (one signed) vertical structure for its eigenvector is the so-called *barotropic* mode which has a shallow water speed of around $200 - 300ms^{-1}$. The other modes are called the *baroclinic* modes and have more complex vertical structures. For the observed stratifications they have much smaller shallow water speeds (the first baroclinic mode has a typical shallow water speed of around $3ms^{-1}$). Because the system here is Sturm-Liouville, the vertical modes satisfy orthogonality conditions. These can be obtained by simple manipulation of the eigenvector equations from equation (7.2.3):

$$\frac{d}{dz} \left(\rho_0 \hat{h}_m \frac{d\hat{h}_n}{dz} - \rho_0 \hat{h}_n \frac{d\hat{h}_m}{dz} \right) = \left(\frac{1}{c_m^2} - \frac{1}{c_n^2} \right) \rho_0 N^2 \hat{h}_m \hat{h}_n$$

If this is integrated from the bottom of the ocean to the top we obtain with the use of the boundary conditions and equations (7.2.2):

$$(7.2.7) \quad \int_0^L \rho_0 N^2 \hat{h}_m(z) \hat{h}_n(z) dz + \rho_0 g \hat{h}_m(L) \hat{h}_n(L) = 0 \quad \text{if } m \neq n$$

From this, the equations (7.2.2) and the boundary conditions we can also obtain by integration by parts that

$$(7.2.8) \quad \int_0^L \rho_0^{-1} \hat{p}_m(z) \hat{p}_n(z) dz = 0 \quad \text{if } m \neq n$$

7.3. An illustrative solution to the vertical equations

To illustrate this system we consider the simplest example in which $N^2 = K^2 = \text{const}$. To further simplify matters we will assume that equation (7.2.6) holds. The solutions then of equation (7.2.3) are obviously sinusoids and cosines however boundary condition (7.2.4) means that only the former are appropriate. We write a general solution then as

$$\hat{h}(z) = h_0 \sin \lambda z$$

subject to the constraint following from the eigenvector equation that

$$(7.3.1) \quad c_n^2 = K^2 / \lambda^2$$

The second boundary condition (7.2.5) when combined with the first equation from (7.2.2) then leads to

$$(7.3.2) \quad c_n^2 \lambda \cos(\lambda L) = g \sin(\lambda L)$$

and then combining (7.3.1) with (7.3.2) leads to

$$(7.3.3) \quad \tan(\lambda L) = \frac{K^2}{\lambda g}$$

which clearly has an infinite set of solutions which are the intersections of the hyperbola $\frac{K^2 L}{(\lambda L)g}$ with the multiple branch function $\tan(\lambda L)$ (see Figure 7.3.1).

Now in general in the ocean $K \sim 10^{-3}$ and $L \sim 4000m$ which means the first solution occurs in a region for which $\tan(\lambda L) \simeq \lambda L$ and other solutions occur for

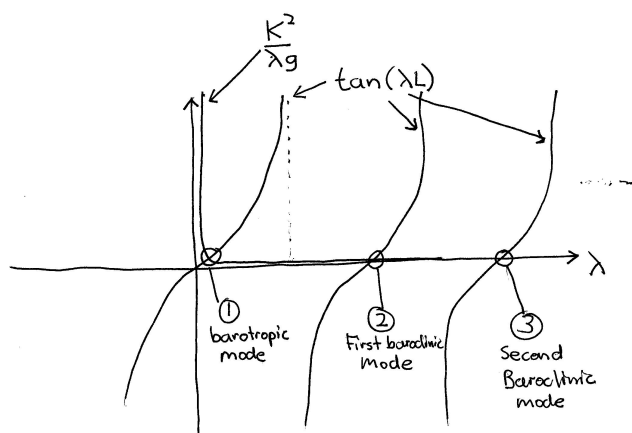


FIGURE 7.3.1. Constant stratification solutions

$\tan(\lambda L) \simeq 0$ (exercise). Thus the first (barotropic) eigenvector and eigenvalue, which we label with a zero subscript, have approximately

$$\begin{aligned}\lambda_0 &= \frac{K}{\sqrt{gL}} \\ c_0 &= \sqrt{gL}\end{aligned}$$

For the parameters chosen above this shows that $c_0 \simeq 200 \text{ms}^{-1}$. Also note that $\lambda_0 \ll L^{-1}$ which shows that the eigenmode has an approximately uniform structure in the vertical. For the other solutions $\lambda L \simeq 0$ implies that $\lambda_n \simeq \frac{n\pi}{L}$ and hence that

$$c_n = \frac{KL}{n\pi} \simeq \frac{1.3}{n} \text{ms}^{-1}$$

Note the $1/n$ dependency of the spectrum for higher order modes. This kind of relation is approximately true for real profiles of N^2 . Note also that the n 'th baroclinic eigenmodes are sinusoids with n nodes and have a vertical velocity at the surface of approximately zero. These properties hold for the "real" modes and the latter is sometimes referred to as the rigid lid approximation (it obviously cannot hold for the barotropic mode). For real profiles the first baroclinic mode is somewhat faster and many of the higher order modes have most of their structure near the surface (see Figure 7.3.2). It is also worth noting that because the baroclinic modes have most of their vertical motion in the interior of the ocean they are sometimes called internal waves while the barotropic mode is sometimes called the exterior mode.

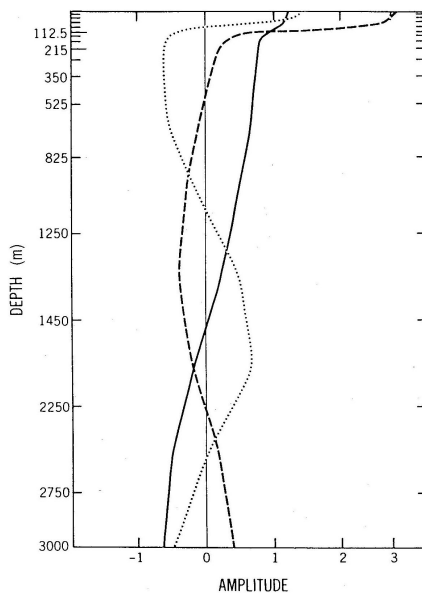


FIGURE 7.3.2. Realistic vertical structure functions for the ocean

7.4. The shallow water equations

Corresponding to the four equations in the vertical (7.2.1) there are a set of equations governing the horizontal flow

$$(7.4.1) \quad \begin{aligned} \frac{\partial U}{\partial t} - fV &= -g \frac{\partial \eta}{\partial x} \\ \frac{\partial V}{\partial t} - fU &= -g \frac{\partial \eta}{\partial y} \\ \tilde{w} &= -H_0 \left(\frac{\partial U}{\partial x} + \frac{\partial V}{\partial y} \right) \\ \tilde{w} &= -\frac{\partial d}{\partial t} = \frac{\partial \eta}{\partial t} \end{aligned}$$

The third and fourth equations here can be combined and a new variable $h \equiv g\eta$ introduced. The resulting equations

$$(7.4.2) \quad \begin{aligned} U_t - fV &= -h_x \\ V_t - fU &= -h_y \\ h_t + c_n^2(U_x + V_y) &= 0 \end{aligned}$$

are commonly referred to as the shallow water equations.

7.5. Wind forced equations

The wind forced linearized momentum equations may be written as

$$\begin{aligned} \frac{\partial u}{\partial t} - fv &= -\frac{1}{\rho_0} \frac{\partial p}{\partial x} + \frac{1}{\rho_0} \frac{\partial X}{\partial z} \\ \frac{\partial v}{\partial t} + fu &= -\frac{1}{\rho_0} \frac{\partial p}{\partial y} + \frac{1}{\rho_0} \frac{\partial Y}{\partial z} \end{aligned}$$

where (X, Y) is the wind stress vector. For the ocean let us assume that the atmospheric stress is deposited into the ocean in an infinitesimal layer of thickness dz near the surface. Actually most is deposited in what is called the mixed layer and we will consider this somewhat more sophisticated model in a later lecture. The basic results however do not change qualitatively. Our momentum equations then become

$$\begin{aligned}\frac{\partial u}{\partial t} - fv &= -\frac{1}{\rho_0} \frac{\partial p}{\partial x} + \frac{1}{\rho_0} X(x, y, t) \delta(z - L) \\ \frac{\partial v}{\partial t} + fu &= -\frac{1}{\rho_0} \frac{\partial p}{\partial y} + \frac{1}{\rho_0} Y(x, y, t) \delta(z - L)\end{aligned}$$

If we expand these equations into vertical modes using the \hat{p}_n then we obtain for the horizontal components

$$(7.5.1) \quad \begin{aligned}\frac{\partial U}{\partial t} - fV &= -g \frac{\partial \eta}{\partial x} + \frac{1}{\rho_0(L)} X \hat{p}_n(L) \\ \frac{\partial V}{\partial t} + fU &= -g \frac{\partial \eta}{\partial y} + \frac{1}{\rho_0(L)} Y \hat{p}_n(L)\end{aligned}$$

The important thing to notice here is that the forcing projects onto the various horizontal equations with a coefficient of $\hat{p}_n(L)$. The value of this coefficient shows quite a strong dependency on stratification structure and so the windstress from the atmosphere excites different vertical modes preferentially in different geographical locations. In the western Pacific the first fastest baroclinic mode is most stimulated. In the eastern Pacific and Atlantic the second baroclinic mode is more stimulated. As these modes have quite different shallow water speeds the dynamical implications can be important.

7.6. Horizontal solutions on the equatorial β -plane

In the tropics it is a reasonable approximation to set the Coriolis parameter $f = 2\Omega \sin \varphi$ to the approximate expression

$$f = \beta y$$

where $\beta = 2.3 \times 10^{-11} m^{-1} s^{-1}$ is exact at the equator and approximately constant for most of the tropics. y is the distance from the equator. The shallow water equations now read

$$(7.6.1) \quad \begin{aligned}U_t - \beta y V &= -h_x \\ V_t + \beta y U &= -h_y \\ h_t + c^2(U_x + V_y) &= 0\end{aligned}$$

These may be reduced to a single equation in V by several lines of manipulation (exercise):

$$(7.6.2) \quad (V_{xx} + V_{yy})_t + \beta V_x - c^{-2} V_{ttt} - \frac{\beta^2 y^2}{c^2} V_t = 0$$

General solutions to these equations can be found by separating variables again and can be written as sums of terms of the form

$$(7.6.3) \quad V = V(y) \exp(ikx - i\omega t)$$

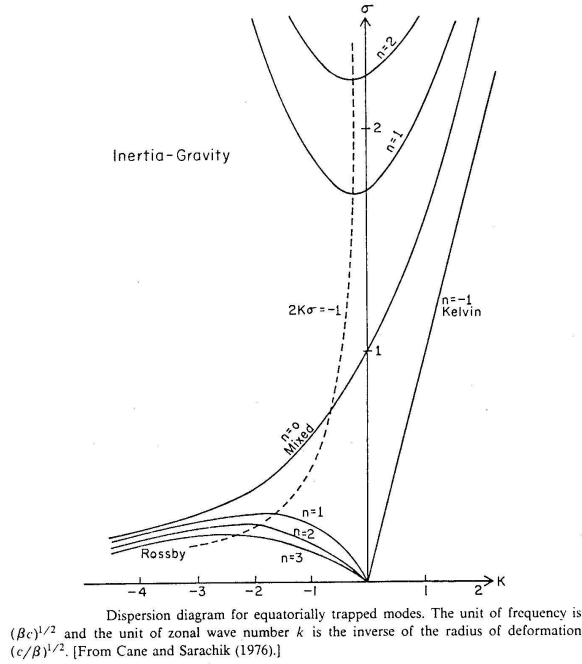


FIGURE 7.6.1.

where we need to derive a dispersion relation for k and ω . Substitution of (7.6.3) into (7.6.2) leads to the equation

$$(7.6.4) \quad V_{yy} + \left(\frac{\omega^2}{c^2} - k^2 - \frac{\beta k}{\omega} - \frac{\beta^2 y^2}{c^2} \right) V = 0$$

Now the operator $-\partial_{yy} + y^2$ is easily shown to be Hermitean and positive and we again have a Sturm Liouville problem this time on an infinite domain. The solutions to this eigenproblem are well known (those of you who have done quantum mechanics will recognize this equation as the Schroedinger wave equation for the harmonic oscillator which has been much studied). The eigenvalues are discrete and (obviously) bounded below and we have

$$(7.6.5) \quad \frac{\omega^2}{c^2} - k^2 - \frac{\beta k}{\omega} = \frac{\beta}{c} (2n + 1) \quad \text{for } n = 0, 1, 2, 3, \dots$$

In addition there is a solution which has $V = 0$. Substitution of this in (7.6.1) gives the dispersion relation $\omega^2 = c^2 k^2$ and the negative root here gives unbounded solutions for U and h as $y \rightarrow \infty$ so we are left with the additional relation

$$(7.6.6) \quad \omega = kc$$

The solutions to both dispersion relations are plotted in Figure 3.

The upper (i.e. high frequency) curves are called gravity waves and are generally unimportant on climate time scales; the curves on the lower left hand side are called

Rossby waves while the curve corresponding to (7.6.6) is for the so-called *Kelvin wave*¹.

The eigensolutions of (7.6.4) (as well as the additional $V = 0$) are the well known *parabolic cylinder functions*

$$(7.6.7) \quad D_n(\xi) \equiv D_n(\sqrt{\beta/cy}) = \exp(-\xi^2/2) H_n(\xi)$$

where $H_n(\xi)$ are the *Hermite polynomials* for which we have the following

$$(7.6.8) \quad \begin{aligned} H_0(\xi) &= 1 \\ H_1(\xi) &= 2\xi \\ H_2(\xi) &= 4\xi^2 - 2 \\ \frac{\partial H_n}{\partial \xi} &= 2nH_{n-1} \\ \xi H_n &= nH_{n-1} + 0.5H_{n+1} \end{aligned}$$

The eigensolutions satisfy the orthogonality relation

$$\int_{-\infty}^{\infty} D_n(\xi) D_m(\xi) d\xi = 2^n n! \pi^{1/2} \delta_{mn}$$

Note that we have introduced a natural scaling distance $a = \sqrt{c/\beta}$ which is known as the equatorial radius of deformation.

The first few parabolic cylinder functions are displayed in Figure 4.

Note that they symmetric (about the equator) for n even and antisymmetric for n odd. Solutions for V are proportional to these functions while the solutions for U and h can be obtained by substituting for the V solution back in (7.6.1) and using (7.6.3), (7.6.8) and (7.6.7):

$$(7.6.9) \quad \begin{aligned} V &= C \exp(ikx - i\omega t) D_n(\xi) \\ U &= C \exp(ikx - i\omega t) \left[\frac{n^{1/2} D_{n-1}(\xi)}{\omega + ck} + \frac{(n+1)^{1/2} D_{n+1}(\xi)}{\omega - ck} \right] \\ h &= C \exp(ikx - i\omega t) \left[\frac{n^{1/2} D_{n-1}(\xi)}{\omega + ck} - \frac{(n+1)^{1/2} D_{n+1}(\xi)}{\omega - ck} \right] \end{aligned}$$

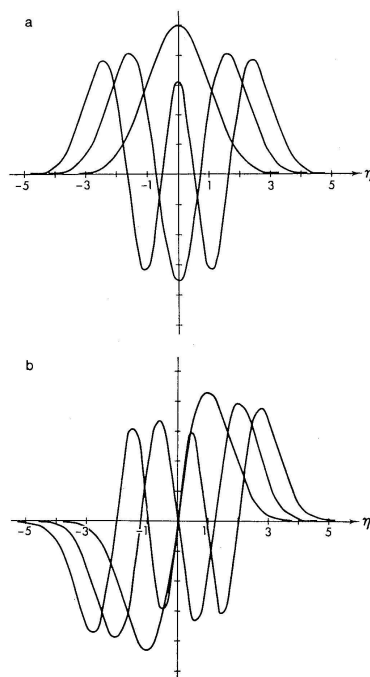
Notice that when U and h are symmetric then V is antisymmetric and conversely. The Kelvin wave solution has $V = 0$ and U and h proportional to $D_0(\xi)$.

7.7. Rossby waves

The low frequency solutions of the dispersion relation (8.2.3) are the Rossby waves and depend for their existence on the fact that the Coriolis parameter varies with latitude (i.e. that $\beta \neq 0$). Their approximate dispersion relation can be obtained by neglecting the term involving ω^2 in (8.2.3) and solving for ω :

$$(7.7.1) \quad \omega = \frac{-\beta k}{k^2 + \frac{\beta(2n+1)}{c}}$$

¹The other solution which has $n = 0$ is called a *mixed Rossby-gravity wave* since it resembles the former for $k \rightarrow -\infty$ and the latter for $k \rightarrow \infty$.



The latitudinal structure of (a) symmetrical and (b) antisymmetrical Hermite functions that describe the meridional velocity component. The unit of distance in the northward direction is the equatorial radius of deformation.

FIGURE 7.6.2.

The limits of $|k|$ small (long waves) and $|k|$ large (short waves) are of significant interest physically. In the former case we can neglect k^2 from the denominator in (7.7.1) and obtain

$$(7.7.2) \quad \omega = \frac{-ck}{2n+1}$$

which is non-dispersive and indicates that these waves propagate towards the west. Note that as n increases this speed slows. The first (or gravest) symmetric Rossby wave has $n = 1$ and the long wave horizontal structure is plotted in Figure 7.7.1.

Note the cyclonic couplet structure. It travels at a speed which is one third of the shallow water velocity. These waves play a fundamental role in equatorial dynamics and can easily be discerned in the observations of the equatorial ocean where they have typical zonal spatial scales of $2000 - 5000 km$. Short Rossby waves play an important role in western boundary currents which we discussed in the previous lecture.

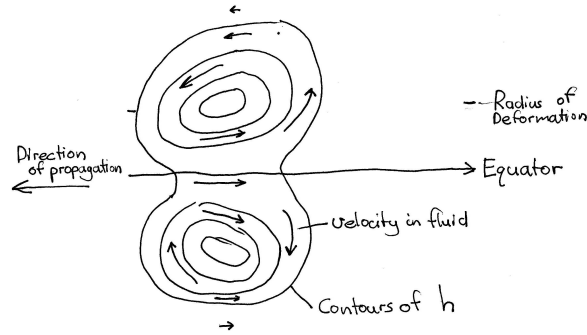


FIGURE 7.7.1. The horizontal pressure structure of the first equatorial Rossby wave

7.8. Kelvin waves

These waves have no meridional velocity and satisfy the non-dispersive relation

$$\omega = kc$$

which means they propagate towards the east with the shallow water speed. Their zonal velocity and h structure is given by simply substituting $V = 0$ into (7.6.1) and using (7.6.3):

$$\begin{aligned} U &= U_0 \exp(ikx - i\omega t) D_0(\xi) \\ h &= cU_0 \exp(ikx - i\omega t) D_0(\xi) \end{aligned}$$

There now exist very good observations along the equator and these waves can be clearly seen propagating most typically with the first baroclinic shallow water speed. Note the Gaussian profile about the equator. These waves, are like long wave Rossby waves, fundamental to equatorial dynamical adjustment.

7.9. Forced equations

As we saw above the effects of wind stress forcing of the ocean can be easily taken into account in the linearized primitive equations by incorporating forcing terms into the shallow water equations which describe the horizontal flow. Thus we have

$$(7.9.1) \quad \begin{aligned} U_t - \beta y V &= -h_x + rX \\ V_t + \beta y U &= -h_y + rY \\ h_t + c^2(U_x + V_y) &= 0 \end{aligned}$$

where (X, Y) is the wind stress forcing. The coefficient r is determined by the projection onto the vertical modes as outlined previously. If we expand (X, Y) in terms of the parabolic cylinder functions discussed in section 6, we can determine the projection onto the various Rossby and Kelvin waves.

7.10. The Sverdrup balance

It is useful to consider steady state solutions of the shallow water equations for wind forcing:

$$(7.10.1) \quad \begin{aligned} -\beta y V &= -h_x + X \\ \beta y U &= -h_y + Y \\ U_x + V_y &= 0 \end{aligned}$$

Differentiating the first equation by y and the second by x and use of the third equation gives the relation

$$(7.10.2) \quad \beta V = Y_x - X_y$$

which is the *Sverdrup balance* seen in previous lectures. A further interesting result is obtained if we consider the case of a constant zonal wind stress (a situation that applies approximately in the equatorial waveguide of the Pacific). Equation (7.10.2) shows that $V = 0$. The third equation of (7.10.1) then shows that U cannot vary zonally which implies it must be zero in a basin situation. The first equation gives the useful relation

$$h_x = X$$

which shows that the slope of the thermocline is proportional to the zonal wind stress. Such a result again is borne out to a surprising degree of accuracy over much of the equatorial ocean. In the Pacific it implies that the thermocline slopes up from west to east and that most of this slope occurs in the central part of the basin where zonal wind stress is greatest. The solutions $(U, V) = 0$ appear less promising and it will turn out that the inviscid balance of equation (7.10.1) is not appropriate for currents where dissipation effects are quite important just as was the case previously when we considered the western boundary region.

7.11. The effects of dissipation

As noted, the final Sverdrup equilibrium when winds are uniform is a state of zero currents. This situation changes dramatically however if dissipation is considered as it must be because of the effects of (mainly) vertical mixing. A simple way to see these effects is to include the so-called ‘‘Rayleigh friction’’ and ‘‘Newtonian cooling’’ into the shallow water set:

$$(7.11.1) \quad \begin{aligned} (\partial_t + \epsilon) U - \beta y V &= -h_x + rX \\ (\partial_t + \epsilon) V + \beta y U &= -h_y + rY \\ (\partial_t + \epsilon) h + c^2(U_x + V_y) &= 0 \end{aligned}$$

For simplicity we are assuming the dissipation coefficients are the same in the first, second and third equations. A useful limit to consider for the damped equations now occurs when the dissipation time scale is short compared to the time scale for boundary effects to influence interior points. The condition for this limit to hold is clearly

$$\epsilon L c^{-1} \gg 1$$

where L is the forcing or basin zonal space scale. In this scenario using the third shallow water equation we obtain the (steady state) scaling equation

$$h_x \sim \frac{-c^2}{\epsilon L} \left[\frac{U}{L} + \frac{V}{L_y} \right] \sim 0$$

Therefore on the equator we obtain from the first shallow water equation the approximate steady state balance is

$$U = \epsilon^{-1} rX$$

showing that in this limit of dissipation strength that the zonal current adjusts directly to the windstress. Here the transient effects of wave propagation that set up the Sverdrup balance between h_x and rX in the inviscid case are ineffective because the waves are strongly damped.

7.12. Multiple vertical mode adjustment

A useful linear model of three dimensional equatorial adjustment was proposed by J. P. McCreary in 1981. As this model used in detail the vertical mode formalism already introduced we consider it in detail. The model used is just the linearized primitive equations but McCreary proposed a simple formulation for the vertical mixing of momentum and temperature which still allowed the vertical mode decomposition. His equations were

$$\begin{aligned} u_t - fv &= -\frac{1}{\rho_0} p_x + (\kappa u_z)_z \\ v_t + fu &= -\frac{1}{\rho_0} p_y + (\kappa v_z)_z \\ g\rho &= -p_z \\ \frac{\partial w}{\partial z} + \frac{\partial u}{\partial x} + \frac{\partial v}{\partial y} &= 0 \\ \frac{\partial \rho}{\partial t} + w \frac{\partial \rho_0}{\partial z} &= (\kappa \rho)_{zz} \end{aligned} \tag{7.12.1}$$

where there is assumed to be no surface density flux and where the definition of wind stress means that at the surface we have

$$\kappa u_z = X/\rho_a \quad \kappa v_z = Y/\rho_a \tag{7.12.2}$$

where (X, Y) is the windstress and ρ_a is the air density. The crucial mathematical choice made by McCreary was to set

$$\kappa = A/N^2 \tag{7.12.3}$$

which is physically plausible because one would expect intuitively that as the stratification increased (i.e. N^2 increased) that turbulence should decrease. It turns out that the discussion below really only depends on the vertical mixing terms being of a generalized Laplacian form in z so this choice is not really important except from a mathematical or expository viewpoint. With this choice the vertical modal

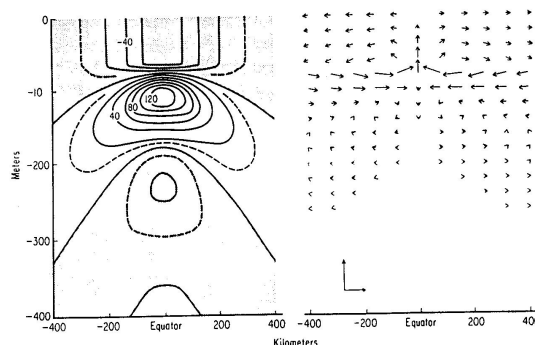


FIGURE 7.13.1. McCreary's model results. Left panel is zonal current. Right panel shows meridional and vertical velocity.

decomposition made in Lecture 3 still holds but now the shallow water equations are modified as follows

$$(7.12.4) \quad \begin{aligned} U_t^n - fV^n &= -h_x^n - \frac{A}{c_n^2} U^n \\ V_t^n + fU^n &= -h_y^n - \frac{A}{c_n^2} V^n \\ h_t^n + c_n^2 (U_x^n + V_y^n) &= -\frac{A}{c_n^2} h^n \end{aligned}$$

Notice that these equations are identical in form with the dissipated shallow water equations (7.11.1) considered in the previous section. The important point here is that the dissipation increases strongly as the shallow water speed of the particular vertical mode decreases or as its mode number increases. Thus as a general rule one will expect that for appropriate (and realistic) choices for A the low order modes will adjust approximately inviscidly while the higher order modes will adjust according to the high dissipation limit discussed in the previous section. This simple observation is enough to explain much of the observed equatorial current and thermocline structure.

7.13. Solutions and Observations

If McCreary's model is spun up then a cross-section across the equator looks like Figure 7.13.1. For comparison Figure 7 shows the observed Pacific current system.

7.14. Non-linear effects

The equatorial current systems of both the Atlantic and Pacific are particularly strong (order $1ms^{-1}$) and as well there is strong equatorial upwelling (order $3 \times 10^{-5}ms^{-1}$) due to surface Ekman divergence about the equator. This means that non-linearity cannot be ignored. Most of the effects are connected with the equatorial undercurrent.

On the equator the most significant non-linearity arises from the zonal momentum advection term

$$wu_z$$

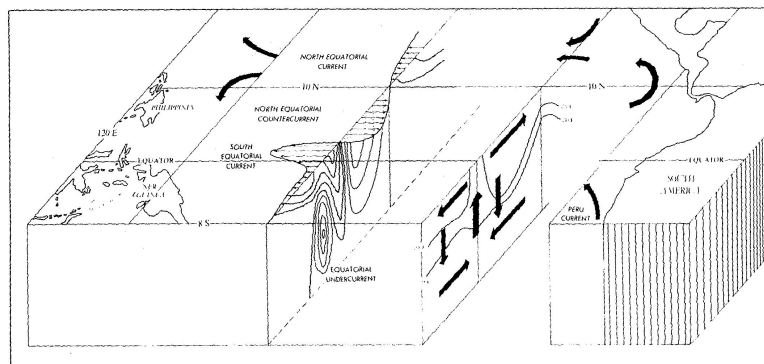


FIGURE 7.13.2. The observed current system for the Pacific Ocean.

For the typical values mentioned above and for vertical depth scales of order $100m$ this term is of order $2 \times 10^{-7} m s^{-2}$. This is enough to accelerate the undercurrent from rest to full strength in around 200 days and therefore cannot be neglected. The primary effect on the linear solution is to import the eastward momentum of the undercurrent into the equatorial surface westward current thereby strongly reducing its strength and thus obtaining better agreement with the observational data.

Off the equator a different term is important: At depth there is convergent flow into the undercurrent and so meridional advection of zonal momentum is important:

$$vu_y$$

The equatorial undercurrent has a typical meridional scale of order $200km$ and meridional currents connected with the overturning cell are of order $0.1 m s^{-1}$. Therefore this term has magnitude around the same as the equatorial vertical advection term (a little thought shows this to be unsurprising). The effect of this term is to shrink the meridional extent of the undercurrent since it has the effect of importing zero velocity off-equatorial water.

7.15. Model Description

An extended version of the McCreary model given by equations (7.12.1) and (7.12.3) is used. Comprehensive documentation may be found in Keenlyside and Kleeman (2002). As noted in the appropriate section above, this form of the equations allows solutions to be decomposed uniquely into a series of vertical modes each satisfying damped shallow water equations of the form (7.12.4). The particular values for the shallow water speeds c_n must be obtained by solving the Sturm Liouville eigensystem (7.2.3), (7.2.4) and (7.2.5). As will be noted from the form of these equations they need a specification of N^2 i.e. the vertical profile of density (stratification). For this model we use observed density data from the equatorial dateline i.e. the central Pacific to define the spectrum of shallow water speeds but used the local stratification data to define the vertical structure functions (i.e. the

eigenvectors) at each horizontal location². Note also from equations (7.5.1) that once we obtain the vertical structure functions (i.e. the eigenvectors) we can also determine how the surface windstress projects onto each of the vertical modes: It depends on the value of the appropriate eigenvector at the surface of the ocean. Once A is specified in (7.12.4) then the dissipation is specified and we can then solve the forced equations providing we have an estimate of the windstress. This we obtain from the annually averaged observations. Small horizontal diffusion terms were also included to improve the smoothness of solutions.

The shallow water equations for each vertical mode are solved in a rectangular box centered on the equator and extending from $125^\circ E$ to $80^\circ W$ and $33.5^\circ S$ to $33.5^\circ N$. The meridional grid resolution in the vicinity of the equator (0.5°) is taken to be sufficiently small to adequately resolve the undercurrent. Realistic land points are included within the rectangular box.

The model also contains two ancillary layers in the upper $125m$ to allow for an Ekman (boundary) flow as well as a crude non-linear correction of the momentum equations in regions where the vertical and meridional advection of zonal momentum is important (see previous section). The first layer is taken to be the upper ocean well mixed layer and its depth varies according to the climatological stratification (the observed annually averaged data is analyzed and the depth for which $N^2 < 6.5 \times 10^{-6} s^{-2}$ is taken as the mixed layer depth). The second layer extends down from the base of the mixed layer to the depth of $125m$.

The Ekman layer flow is incorporated to simulate the neglected/truncated higher vertical modes. Such modes have much of their structure near the surface and because of the form of equation (7.12.4) are highly dissipated relative to the lower order vertical modes. Due to this high dissipation it turns out we can neglect the time tendency, pressure gradient as well as horizontal diffusion terms for each mode. Once these terms are neglected an explicit solution can be found for all the neglected modes at all levels. This is integrated across the two layers and added as a bulk quantity to the two ancillary layers.

Non-linear momentum effects are obtained by returning to equations (7.1.1) and (7.1.2) and adding the appropriate advection terms to the zonal momentum equation. It is assumed that the meridional non-linear piece is small which can be verified in more complete primitive equation simulations. We then split the zonal flow into a linear piece which satisfies the usual equations already discussed and a residual non-linear piece which is driven by the added advection terms. A prognostic equation for the non-linear zonal current then results and this is integrated across the two ancillary layers. The continuity equation (7.1.2) also allows us to compute the non-linear contribution to the vertical velocity between the two ancillary layers.

²This approximation is discussed at length in Keenlyside and Kleeman (2002). It has the effect of improving the vertical appearance of currents but has little effect on the dynamics.

7.16. Model Interface

As before a matlab graphical user interface is provided to facilitate rapid and instructive running of the model detailed in the last section. An example configuration of this is shown in Figure 7.16.1.

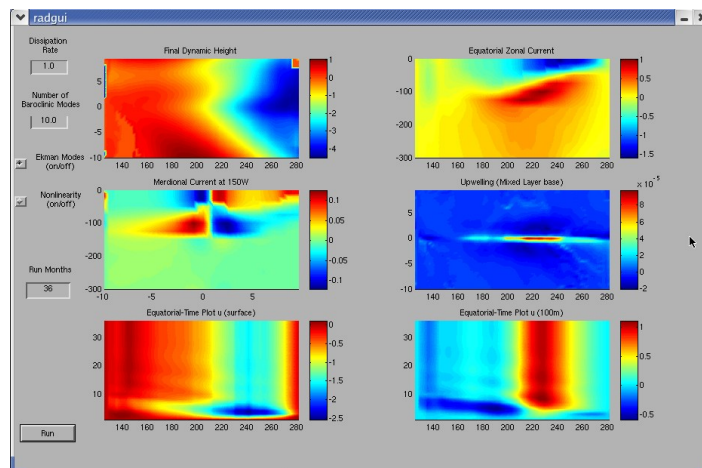


FIGURE 7.16.1. The graphical user interface for the undercurrent model. Results from a typical model run are displayed.

As in previous chapters **ensure that all parameter values including the radio button on/off switches are reset before running the model.** The model runs forward from a state of rest. The model parameters are detailed in Table 1.

The panels have the following meanings:

Top left: Longitude-Latitude plot of the dynamic height (surface pressure) at integration end.

Top right: Longitude-depth plot along the equator of zonal current at integration end.

Center left: Latitude-depth plot along $150^{\circ}W$ of meridional current at integration end.

Center right: Longitude-Latitude plot of vertical velocity at mixed layer base and at integration end.

Bottom left: Longitude-time plot of surface zonal current along the equator.

Bottom right: Longitude-time plot of zonal current at depth of $100m$ along the equator.

The model is intended to be run for a maximum of 3 years and the time panels only extend that far. In general for a sensible choice of A the model is then close to a steady state.

Model Parameter	Parameter meaning
Dissipation rate	Controls the value of A linearly. A value of 1.0 gives a reasonable simulation
Number of Baroclinic modes	Number of vertical modes to retain
Ekman Modes (on/off)	Decides whether to add the Ekman flow
Non-linearity (on/off)	Decides whether to add the non-linear zonal flow
Run months	Number of months to integrate model Note that a maximum of 36 only are displayed

TABLE 1. Equatorial undercurrent model parameters